

Design of Criticality-Based Haptic Steering Guidance for Human Like Adaptation to Different Lane Keeping Tasks

Sjors Oudshoorn, Sarvesh Kolekar, and David Abbink, *Senior Member, IEEE*

Abstract—Haptic steering guidance is an advanced driving assistance system which provides guidance torques on the steering wheel to assist a human driver. Improvements in performance, safety margins and workload have been reported for lane-keeping and curve negotiation tasks. On the other hand, the guidance system instigates increased driver torques, indicating the occurrence of a mismatch between driver and automation intention. A novel, criticality-based control structure was developed, capable of adapting to different driving conditions by using safety margins (operationalized as time-to-line crossing, TLC) as input. Twenty-four participants drove through a single-lane, 10.8 km long road, with as independent variables the road width (normal road width of 3 m, wide road width of 5 m) and the type of guidance received: no guidance (manual), haptic steering guidance based on lateral deviation from the center-line (performance-based guidance, PBG) and criticality-based guidance (CBG). On the normal road, results show similar benefits for both guidance systems compared to manual control, in terms of performance and safety margins. Workload was reduced by PBG, but both guidance systems yielded increased driver torques. On the wide road, participants drove closer to the center-line with PBG, but at the cost of significantly more guidance torques than CBG. Interestingly, this reduction in lateral deviation did not result in a significant improvement for lowest safety margins encountered. No subjective preference was found for either feedback condition. It can be concluded that criticality-based guidance is capable of adjusting to different driving conditions, without compromising safety margins, whilst greatly reducing guidance torques in situations where they are unneeded.

Keywords—Haptic steering guidance, TLC, guidance-as-needed, human-automation interaction.

I. INTRODUCTION

Haptic shared control has been proposed as a viable alternative to complete automation for multiple applications, such as surgery (Okamura and Li, 2003; Nudehi et al., 2005), teleoperation (Sheik-Nainar et al., 2005) and vehicle operation (Griffiths and Gillespie, 2004; Forsyth and MacLean, 2006; Mars et al., 2014) due to improved human operator engagement (Abbink et al., 2011). For the latter, a human driver and an intelligent automated system cooperatively guide the vehicle over the road. The haptic interface, an actuated steering wheel to provide haptic steering guidance for lateral control (Mulder et al., 2012) or an actuated gas pedal for longitudinal control (Mulder et al., 2011), facilitates communication between the two agents, by providing guidance torques determined by the automation to the human operator (Abbink and Mulder, 2009). The system requires continuous input of the driver,

whilst simultaneously providing continuous feedback of automation state functionality; this promotes driver engagement and improves system transparency (Abbink et al., 2011). In lane keeping and curve negotiation tasks, studies have shown that lateral error (with respect to the lane center line) has decreased (Mohellebi et al., 2009; Saleh et al., 2013; Forsyth and MacLean, 2006; Mulder et al., 2008), driver workload has been reduced (Van Der Horst, 2004; Mars et al., 2014), and safety margins, in terms of time-to-line crossing (TLC) have improved (Melman et al., 2017) when driving with haptic steering guidance, compared to manual driving. Additionally, efforts have been made to support other aspects of the driving task, such as velocity control (Mulder et al., 2011), obstacle avoidance (Della Penna et al., 2010), lane changes (Tsoi et al., 2010) and overtaking (Flemisch et al., 2014). However, the aforementioned benefits of haptic steering guidance come at the cost of additional torques exerted by the driver, which can increase by a factor of up to three (Tsoi et al., 2010; Mars et al., 2014).

These increased driver torques have been argued to be a result of conflict between the driver and the haptic guidance system (Mars et al., 2014). Conflict arises when a mismatch occurs between driver and automation, in determining the course of action at a given driving scenario; it has been reported in a simulator study that participants had to 'fight' the controller (Abbink et al., 2011), which can worsen the overall performance (Mars et al., 2014; Griffiths and Gillespie, 2004). Conflicts can occur both within a task (e.g. lane keeping; Petermeijer et al., 2014), as well as when switching between tasks (e.g. from lane keeping to lane changing; Tsoi et al., 2010). Moreover, driver torques tend to increase as the level of haptic authority (the magnitude of the guidance torques) increases (Mars et al., 2014). In order to prevent conflict and thereby reduce driver torques, the intention of the automation needs to more closely match that of the driver.

Most of the current haptic steering guidance systems for lane keeping minimize either the lateral deviation from the lane center line (Griffiths and Gillespie, 2004), the error between vehicle and road heading (Mohellebi et al., 2009), or a combination of both (Abbink and Mulder, 2009; Saleh et al., 2011). The resultant guidance system operates as an optimizing controller. However, it has been argued that operators act as a satisficer, aiming to fulfill safety thresholds (Goodrich et al., 2000), and thus that the support system should act similarly (De Winter and Dodou, 2011). This was investigated by De Groot et al. (2011), who administered seat vibrations when the lateral error surpassed a safety limit, and by Petermeijer et al. (2014), who developed a bandwidth controller which used the same safety limit to provide guidance torques on the

All authors are with the Department of Biomechanical Engineering, Faculty of 3mE, Delft University of Technology, Mekelweg 2, 2628 CD Delft, The Netherlands. Email: s.r.f.oudshoorn@student.tudelft.nl.

steering wheel, guiding the driver back to the lane center line. However, Boer (2016) argued that evaluating and controlling for lateral deviation is not a direct representation of driver decision making; instead, drivers adjust their trajectory based on maintaining safety margins, in terms of time constraints (Van Winsum and Godthelp, 1996).

In lane keeping and curve negotiation tasks, (TLC) serves as a measure of situational criticality (Van Winsum et al., 2000; Saleh et al., 2013). It is a metric for lateral control of the vehicle; its counterpart for longitudinal control, time-to-collision, has successfully been used to provide guidance on a haptic gas pedal (Mulder et al., 2011) and in obstacle avoidance systems (Della Penna et al., 2010), providing benefits in driver vigilance. To the best of our knowledge, no previous efforts were made to assist drivers in a lane keeping task by evaluating and controlling for TLC in a haptic steering guidance system. Guidance will be provided based on criticality of the vehicle trajectory. As TLC incorporates upcoming road curvature, lane width, velocity, vehicle orientation and steering wheel angle, it allows for adaptation to different driving tasks, comparable to the behavioral changes of human drivers as task requirements change (Zhai et al., 2004; Van Winsum and Godthelp, 1996).

Although the potential benefits of the use of time-to-line crossing in haptic steering guidance are promising, its use in a control structure, rather than as an evaluation metric, is subject to limitations. It is a non-linear parameter, with discontinuities when the lane boundary to be crossed switches (Van Winsum et al., 2000). As the vehicle approaches the lane boundary, small steering corrections can inflate (or deflate) the measured criticality. Moreover, TLC by itself is non-descriptive; whilst it offers quantification of criticality, it does not inherently offer a direction to adjust the trajectory towards.

In this paper, a control structure is proposed to alleviate the aforementioned limitations of TLC, by means of incorporating human-like uncertainty around the current trajectory, generating a field of safe travel (Boer, 2016). Parameters were identified in comparison to human driving data. A trigonometric approach for TLC computation is elaborated (Van Winsum et al., 2000), and a driving-simulator study is conducted to evaluate the benefits and limitations of the developed criticality-based haptic steering guidance, in comparison to a previously studied performance-based guidance system (Mulder et al., 2012), on two different road widths, of 3 m and 5 m respectively; the difference in road width directly influences corresponding safety margins, thereby adjusting the preferred trajectories of human drivers (Van Winsum and Godthelp, 1996).

II. TIME-TO-LINE CROSSING

A. Trigonometric TLC Computation

In this paper we present an extension of the trigonometric approach of TLC calculation, based on derivation from Boer, 2016; Van Winsum et al., 2000. In previous studies, time-to-line crossing was used for evaluation of safety margins (Saleh et al., 2013). For this end, Van Winsum et al. (2000) developed an approximation, which greatly simplified the TLC calculation:

$$TLC_{approx} = \frac{y}{\dot{y} + \ddot{y}} \quad (1)$$

With $y [m]$ the margin until lane boundary (perpendicular to the lane), and $\dot{y} [ms^{-1}]$ and $\ddot{y} [ms^{-2}]$ the corresponding lateral velocity and lateral acceleration, respectively. Whilst its use for evaluation of safety is successful, the simplifications make it unsuited for use as control input (for example, upcoming road profile is not taken into account); therefore, the trigonometric approach will be used, to offer accurate, reliable and robust calculation (Boer, 2016; Van Winsum et al., 2000).

A trigonometric TLC calculation requires consideration of four different scenarios: driving with either a straight (steering wheel angle = 0) or curved vehicle trajectory (steering wheel angle $\neq 0$), on either a straight or curved road section. The vehicle drives with a velocity $v [m \cdot s^{-1}]$; furthermore, steering wheel angle and velocity are assumed constant.

1) *Straight road, straight trajectory*: Driving on a straight road with a straight vehicle trajectory is depicted in figure 1a. The vehicle has $y [m]$ margin to the lane boundary (measured from front left or front right wheel), with heading error $\alpha [^\circ]$ between road heading and vehicle heading.

$$TLC = \frac{y \cdot \sin(\alpha)}{v} \quad (2)$$

2) *Straight road, curved trajectory*: When steering input is not equal to 0, the vehicle follows a curved trajectory, with yaw rate $\dot{\psi} [rad \cdot s^{-1}]$ (for the relation between yaw rate and steering wheel angle, see Appendix A). The yaw rate is used to determine vehicle curve radius R_v :

$$t_{circ} = \frac{2\pi}{\dot{\psi}} [s] \quad (3)$$

$$d_{circ} = t_{circ} \cdot v [m] \quad (4)$$

$$R_v = \frac{d_{circ}}{2\pi} = \frac{v}{\dot{\psi}} [m] \quad (5)$$

Referring to figure 1b:

$$A = \frac{y}{\cos(\alpha)} \quad (6)$$

$$B = R_v - A \quad (7)$$

$$\beta = 90 + \alpha \quad (8)$$

In order to compute φ , length C needs to be determined. Applying the cosine rule for side R_v :

$$R_v^2 = B^2 + C^2 - 2B \cdot C \cdot \cos(\beta) \quad (9)$$

Rewriting and solving for side C:

$$C = \frac{2B \cdot \cos(\beta) \pm \sqrt{(2B \cdot \cos(\beta))^2 - 4(B^2 - R_v^2)}}{2} \quad (10)$$

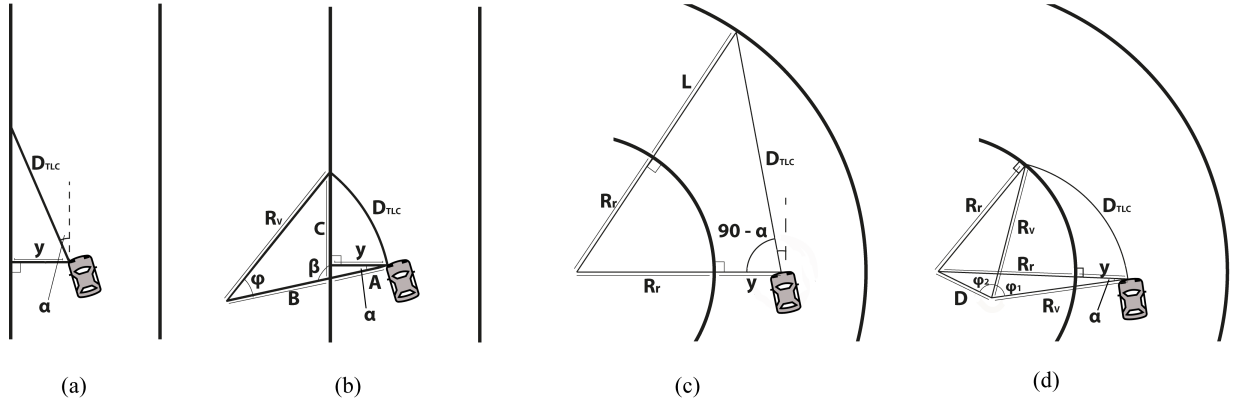


Fig. 1: TLC calculation for straight and curved road sections. All depicted vehicle trajectories D_{TLC} are at constant velocity and steering wheel angle. (a) the simplest scenario: driving on a straight road with no steering input, at heading error α and lane margin y ; (b) steering action is incorporated, visualized as vehicle curve radius R_v ; (c) the scenario of driving on curved road, with inner road curve radius R_r and lane width L , without steering input; (d) driving through a curve with steering input.

Again applying the cosine rule to solve for φ and determine the corresponding arc length:

$$\varphi = \arccos\left(\frac{B^2 + R_v^2 - C^2}{2B \cdot R_v}\right) \quad (11)$$

$$D_{TLC} = \varphi \cdot R_v \quad (12)$$

$$TLC = \frac{D_{TLC}}{v} \quad (13)$$

It should be noted that the vehicle trajectory can be directed towards either increasing heading error (as was depicted in figure 1b), or towards decreasing heading error (i.e. vehicle oriented towards the left boundary, but with steering towards the right). Two additional scenarios can therefore be identified: steering correction is either insufficient to prevent the lane crossing (i.e. oriented towards the left, steering towards the right, but crossing the left lane boundary) or sufficient (same situation, crossing the right boundary). Appropriate changes for lane margin y need to be made.

3) *Curved road, straight trajectory*: On a curved road, calculations are more complicated, due to the effect of inner curve radius R_r . Driving on a curved road with a straight vehicle trajectory is depicted in figure 1c. The law of cosines is applied to calculate D_{TLC} , similar to equations 9 and 10. Included in the calculation are heading error α , lateral lane margin y , lane width L and inner curve radius R_r :

$$\beta = 90 - \alpha \quad (14)$$

$$A = R_r + y \quad (15)$$

$$B = R_r + L \quad (16)$$

$$B^2 = A^2 + D_{TLC}^2 - 2A \cdot D_{TLC} \cdot \cos(90 - \alpha) \quad (17)$$

$$D_{TLC} = \frac{2A \cos(\beta) \pm \sqrt{(2A \cos(\beta))^2 - 4(A^2 - B^2)}}{2} \quad (18)$$

$$TLC = \frac{D_{TLC}}{v} \quad (19)$$

Vehicle trajectory can cross either the inner lane boundary, or the outer lane boundary (as visualized in figure 1c). If vehicle trajectory is oriented towards an inner lane boundary crossing, lane width L is excluded from further calculation.

4) *Curved road, curved trajectory*: The final aspect of TLC calculation is a curved trajectory on a curved road, as visualized in figure 1d. It requires the calculation of φ_1 , through means of computing φ_2 and combined angle φ_{12} .

$$D = \sqrt{(R_r + y)^2 + R_v^2 - 2(R_r + y) \cdot R_v \cdot \cos(\alpha)} \quad (20)$$

With D the distance between the center of R_r and R_v . Repeating the law of cosines twice, for φ_{12} and φ_2 :

$$\varphi_{12} = \arccos\left(\frac{D^2 + R_v^2 - (R_r + y)^2}{2R_v \cdot D}\right) \quad (21)$$

$$\varphi_2 = \arccos\left(\frac{D^2 + R_v^2 - R_r^2}{2R_v \cdot D}\right) \quad (22)$$

$$\varphi_1 = \varphi_{12} - \varphi_2 \quad (23)$$

$$D_{TLC} = \varphi_1 \cdot R_v \quad (24)$$

$$TLC = \frac{D_{TLC}}{v} \quad (25)$$

The considerations of both previous sections are relevant here. Calculation is altered when vehicle trajectory will cross the outer lane boundary: lane width L is added to road curve radius R_r . If vehicle heading is also oriented towards the outer lane boundary, the following equations are used for φ_{12} and φ_2 :

$$\varphi_{12} = \arccos\left(\frac{D^2 + R_v^2 - (R_r + L)^2}{2R_v \cdot D}\right) \quad (26)$$

$$\varphi_2 = \arccos\left(\frac{D^2 + R_v^2 - (R_r + y)^2}{2R_v \cdot D}\right) \quad (27)$$

B. Haptic Steering Guidance Design

Three driving conditions were evaluated; manual driving, driving with performance-based guidance and criticality-based guidance. All three conditions provided a light centering stiffness, whilst the latter two provided additional, superimposed haptic guidance torques.

1) *Performance-based Steering Guidance (PBG)*: The PBG system was used previously by Mulder et al. (2012) and Melman et al. (2017), amongst others, and was referred to as continuous guidance. However, to avoid confusion with the newly developed (continuous) guidance system, naming was changed to reflect the main difference: controlling for either lateral error (a measure of performance) or TLC (measure of criticality).

PBG controls for two parameters, predicted lateral error $e_{future,lat}$ and predicted heading error $e_{future,heading}$ at look-ahead time $t_{lha} = 0.7s$ from now, assuming continued driving given the current vehicle and steering wheel state. Guidance torques $T_{guidance}$ were calculated using PD-control, see equation 28:

$$T_{guidance} = (e_{future,lat} \cdot P + e_{future,heading} \cdot D) \cdot K_{pbg} \quad (28)$$

Here, $e_{future,lat}$ is defined as positive leftwards of lane centerline, $e_{future,heading}$ as positive leftwards of 0° heading error and $T_{guidance}$ as positive in rightwards steering corrections (clockwise). Feedback tuning is equal to Mulder et al. (2008) with $P = 0.9$, $D = 0.08$ and $K_{pbg} = 2$.

2) *Criticality-based Steering Guidance (CBG)*: Time-to-line crossing approaches 0 s at increasingly risky driving situations. Equation 29 is used to generate a usable error signal:

$$\Delta e = \frac{TLC \cdot \gamma + \theta}{TLC \cdot \frac{\gamma}{\phi} + 1} \quad (29)$$

Here we have:

$$\lim_{TLC \rightarrow \infty} \Delta e = \phi, \quad \lim_{TLC \rightarrow 0} \Delta e = \theta \quad (30)$$

As such, ϕ and θ determine lower and upper bounds of criticality, respectively. Finally, γ is related to relative weighing between these two bounds. The presence of noise (motor, sensory, neural noise or external noise) influences driving behavior (Kolekar et al., 2016); to illustrate, drivers usually stay away from the edge of the road, regardless of their accuracy in following the road heading. To account for this noise, the impact of any possible disturbance on safety margins is taken into account. In accordance with Boer (2016), current

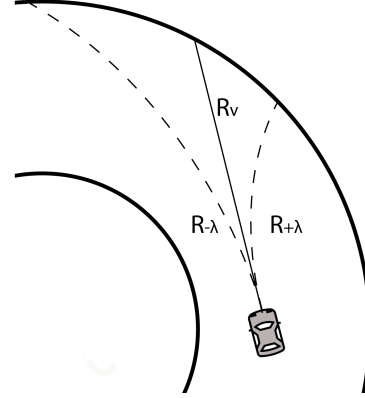


Fig. 2: Vehicle trajectory R_v (steering wheel angle = 0°) with left uncertainty boundary $R_{-\lambda}$ and right uncertainty boundary $R_{+\lambda}$

vehicle curve radius R_v is disturbed with a factor $\lambda[m^{-1}]$ (figure 2):

$$R_\lambda = \frac{1}{R_v^{-1} \pm \lambda} \quad (31)$$

Driving straight (effectively with $R_v = \infty$) yields two uncertainty trajectories with $R_\lambda = \pm \lambda^{-1} [m]$. Conversely, on curved trajectories λ is linearly related vehicle curvature (Boer, 2016).

For both uncertainty trajectories, with vehicle curve radius $R_{-\lambda}$ and $R_{+\lambda}$ respectively (figure 2), corresponding TLC was computed. Combining equations 29 and 31 yields equation 32: the control structure for determining guidance torques $T_{guidance}$ [Nm].

$$T_{guidance} = K_{cbg} \left(\frac{TLC_{-\lambda} \cdot \gamma + \theta}{TLC_{-\lambda} \cdot \frac{\gamma}{\phi} + 1} - \frac{TLC_{+\lambda} \cdot \gamma + \theta}{TLC_{+\lambda} \cdot \frac{\gamma}{\phi} + 1} \right) \quad (32)$$

Driving situations with equal $TLC_{-\lambda}$ (leftwards uncertainty boundary) and $TLC_{+\lambda}$ (rightwards uncertainty boundary) will provide zero control input. As driving situation changes (as visualized in figure 3 as function of lateral error), corresponding $TLC_{-\lambda}$ and $TLC_{+\lambda}$ are evaluated and appropriate $T_{guidance}$ is determined. A clear difference can be seen in guidance system response for increased lane width: PBG increases the maximum guidance torque, whereas CBG widens the range of guidance torque; only close to the lane boundary are torques rapidly increased.

3) *Parameter identification*: In order to support human driving, the output trajectory of the model was compared to experimental results from a simulator study in which participants navigated six curves (inner curve radius 150, 200 and 300 m, left and right) without steering assistance (De Nijs, 2011). The four control parameters (ϕ , θ , γ , and λ) were identified in a simulated driving task: a comparison was

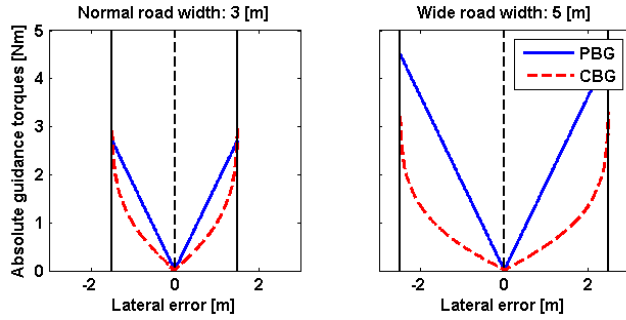


Fig. 3: Magnitude of guidance torques, plotted as function of lateral error, on a straight road, at velocity $v = 130$ km/h, heading error $\alpha = 0$, and yaw rate $\dot{\psi} = 0$. Performance-based guidance (PBG, blue) and criticality-based guidance (red, CBG) are determined for road width = 3 m (left) and road width = 5 m (right)

made between controller trajectory (without human input), and recorded human driver trajectory (without controller input), using variance-accounted for (VAF):

$$VAF = \left(1 - \frac{\sum_i (u_{h,i} - u_{m,i})^2}{\sum_i u_{h,i}^2}\right) * 100 [\%] \quad (33)$$

Here, u_h is the human driver data and u_m represents model data, at time step i . A close match in predicted steering wheel angle (VAF up to 99.01 %) was discovered, but less so for predicted lateral error (VAF up to 47.44 %), which is in accordance with Kolekar et al. (2016). Please refer to Appendix B for a detailed overview.

Parameters were subsequently experimentally adjusted to provide a suitable level of haptic authority for cooperative driving (Mars et al., 2014). Parameter identification yielded $\phi = 0.01$ for lower limit control activity, $\theta = 10$ for upper limit control activity, $\gamma = 0.1$ for relative criticality weighing and $\lambda = 0.004 [m^{-1}]$ for driver uncertainty. Finally $K_{cbg} = 0.3$, the error-to-torque gain, was identified to provide equal level of haptic authority to the aforementioned performance-based guidance, on a normal road. Supplementary sensitivity analysis and simulation structure are included in Appendix B.

III. METHOD

A. Participants

24 subjects, drawn from the Delft student population, participated in the experiment (mean age 24.1, SD 1.9, 16 male). Driving frequency (11 less than once a month, 10 once a month to once a week, 2 one to three days a week, 1 four to six days a week) and average annual driving distance (11 between 1-1.000 km, 7 between 1.001-5.000, 4 between 5.001-10.000, 1 between 10.001-15.000, 1 between 15.001-20.000) were reported by participants. Each participant filled an informed consent form; participation was strictly voluntary, without monetary or other compensation. All participants had normal or corrected to normal eyesight, and were in possession of a valid driver's license for at least one year.

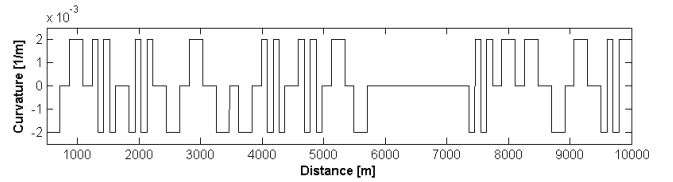


Fig. 4: Road curvature profile for all conditions

B. Apparatus

This study was conducted on a fixed-base simulator; the setup has previously been used by (Mulder et al., 2012; Petermeijer et al., 2014; Melman et al., 2017), amongst others. A dedicated computer controlled a Moog-FCS ECol8000 S-motor, to provide actuation on the steering wheel at 2500 Hz. The visual environment was updated at 60 Hz; three DLP projectors were used to provide 180° horizontal and 40° vertical field of view. A single-track model was used for vehicle dynamics of a heavy sedan. An automated gearbox was used, and velocity was fixed at 130 km/h. A light centering stiffness, as function of the steering wheel angle, was applied in all conditions to emulate wheel-ground interaction forces.

Vehicle orientation with respect to the road, steering wheel angle, velocity and acceleration, driver torques and feedback torques were all recorded at 100 Hz.

C. Road Environment

The participants drove the vehicle over a 10.8 km long, single lane road without other traffic, for approximately 290 seconds. A start and end section, both 500 m long, were used for acceleration and deceleration, and were excluded from subsequent analysis. The road was composed of straights (length 220 meters), left and right single curves (length 218 meters, inner curve radius 500 meters) and winding sections (four alternations, inner curve radii 500 meters, both left first and right first). Curves were interspersed with straight sections (length 150 meters) to prevent crossover effects. See figure 4 for a visualization. The curvature profile was repeated for the training run and normal road-width trial (3 meters road width for both) and wide road-width trial (5 meters road width). A long straight section was included to investigate steady-state behavior. Main analysis was conducted over the entire road; additional comparisons were made between steady state behavior on straight sections (75 meters, 2 seconds) and for curve negotiation (218 meters curved road, as well as 70 meters straight curve entry and curve exit).

D. Experimental Design

All participants read the experiment instructions, signed the informed consent form and reported driving frequency and annual mileage. Participants were orally reminded that they are free to pause or stop the experiment if nausea arises, and task instructions were repeated. Participants were reminded that velocity was fixed at 130 km/h, with automatic acceleration, gear shifts and deceleration, thereby limiting the task to lateral lane keeping and curve negotiation. Participants were

subsequently instructed to drive as they normally would, and were informed that no other road users would be encountered during the trials.

The three assistance conditions (manual, PBG, CBG) were presented to participants in a counterbalanced, within-subjects design; every specific guidance order was encountered by four participants. Each feedback condition was repeated three times: one training run (normal road, 3 meters wide) and two trials (normal road and wide road, 5 meters wide). The order of both trials was counterbalanced over all participants; each specific order was presented three times.

Participants were encouraged to develop an understanding of vehicle dynamics and guidance torques during the training runs. No questions regarding specific controller functionality were answered. After each trial, NASA Task Load Index (NASA-TLX) forms were filled out to assess subjective workload (Hart and Staveland, 1988). Subsequently, participants were inquired for their nausea with a six item question, ranging from not experiencing any nausea (1) to vomiting (6). The experiment would be stopped if any participant responded with a nausea level of 4 or higher; this did not occur throughout the experiment. After trials in which steering assistance was presented, participants were inquired for their acceptance of the assistance system, through means of a five point scale containing nine items (five related to usefulness, four to satisfaction) (Van Der Laan et al., 1997). After each guidance condition, consisting of three experimental runs of approximately 20 minutes, a five minute break was taken.

E. Dependent Measures

Metrics were grouped in performance, safety, workload and acceptance, in accordance with previous research (Petermeijer et al., 2014; Melman et al., 2017).

1) Performance:

- Mean absolute lateral error [m]: a measure of lane keeping accuracy throughout the task;
- Peak absolute lateral error [m]: largest excursion of the driving task.

2) Safety margins:

- Median time-to-line crossing [s]: a measure of safety margins throughout the driving task;
- Minimum time-to-line crossing [s]: indication of the most critical event encountered in each driving task.

3) Workload:

- NASA-TLX score [%]: subjective measure of workload;
- Steering Wheel Reversal Rate (SWRR) [s^{-1}]: number of steering wheel velocity sign changes;
- Mean absolute feedback torques [Nm]: level of assistance received;
- Mean absolute driver torques [Nm]: applied torques by the driver, measure of his effort.

4) System Acceptance:

- Mean driver usefulness and satisfaction [-]: the driver acceptance questionnaire was used to quantify driver acceptance of the support system (Van Der Laan et al., 1997). Five usefulness and four satisfaction items were

rated on a 5-point Likert scale, -2 to +2. Items 3, 6 and 8 were reversed; corresponding sign changes were made in subsequent analysis.

F. Statistical Analyses

Data was analyzed by application of 2-way, repeated measures analysis of variance (ANOVA); independent measures are the guidance condition (manual, PBG, CBG) and the lane width (normal, wide). Significance levels were set at $\alpha = 0.05$.

Post-hoc analysis was conducted by performing pairwise comparisons between guidance conditions on the normal road, between guidance conditions on the wide road, and between road width for all three guidance conditions. Bonferroni correction was applied to adjust α to the nine pairwise comparisons. No results were collected for manual driving for feedback torque, system acceptance and system satisfaction; hence, only four pairwise comparisons were made.

Comparisons were made between left curves and right curves. A 2-way repeated measures ANOVA, with factors driving condition (6) and curve direction (2) was conducted for all 24 participants. A significant result for the factor curve direction indicates a difference in driving strategies for left and right curves.

IV. RESULTS

Table 1 contains statistical results of the investigated dependent measures, taken over the entire road. Reported are the mean and standard deviation for each driving condition, p and F value of the 2-way repeated measures ANOVA (for guidance condition, road width and interaction effects), and significance of pairwise comparisons. Individual statistical results of pairwise comparisons are given in Appendix C. Mean variables for driving on the wide road, as function of road distance (with the curvature profile of figure 4), are visualized in figure 9: PBG drove closest to lane centerline (top subfigure); TLC profiles for all conditions showed comparable peaks (second subfigure; note that between 6000 and 7000 m, TLC was higher than 5 s); guidance torques were lower for CBG for most of the task (third subfigure); both PBG and CBG increased driver torque (bottom subfigure). Figure 8 visualizes individual mean results, as well as the mean over all subjects, for: mean absolute lateral error, minimum TLC, mean absolute feedback torque and mean absolute driver torque. All results are visualized separately for straight and curved road sections, to investigate effect on lane keeping (straight) and curve negotiation (curves).

In Appendix C, the results of the 2-way repeated measures ANOVA, with factors driving condition and curve direction are given. For each of the metrics, analysis yielded a statistically significant difference for the factor curve direction. However, due to raw data showing similar trends, curve data was grouped in all figures to avoid unnecessary clutter. Note that reported statistical analyses only compare data over the entire road.

TABLE I: 2-way Repeated measures ANOVA, with factors lane width (normal, wide) and guidance condition (manual driving, PBG, CBG). Mean and standard deviation per condition are given, as well as statistical result for both factors and interaction. Pairwise comparisons that are significantly different are marked with x.

Variable name	Road width 3 [m] - mean and (SD)			Road width 5 [m] - mean and (SD)			2-way ANOVA - F(2,67)		Pairwise comparison (x = significant)									
	Manual (1)	PBG (2)	CBG (3)	Manual (4)	PBG (5)	CBG (6)	p_{guid} (F)	p_{width} (F)	1-2	1-3	2-3	4-5	4-6	5-6	1-4	2-5	3-6	
<i>Performance:</i>																		
Mean abs lateral error [m]	0.2838 (0.0716)	0.2027 (0.0541)	0.2148 (0.0538)	0.4150 (0.0838)	0.2925 (0.0892)	0.3564 (0.1176)	9.07 · 10 ⁻¹² (46.48)	4.77 · 10 ⁻¹⁰ (105.09)	x	x		x	x	x	x	x	x	x
Peak abs lateral error [m]	1.0834 (0.2458)	0.7768 (0.2008)	0.8452 (0.1389)	1.4392 (0.4091)	1.0541 (0.2822)	1.2043 (0.3577)	3.93 · 10 ⁻¹¹ (42.18)	1.75 · 10 ⁻⁶ (40.38)	x	x		x	x		x	x	x	x
<i>Safety:</i>																		
Median TLC [s]	2.0500 (0.1115)	2.1837 (0.1081)	2.1356 (0.0901)	2.7562 (0.1397)	2.8606 (0.1062)	2.8142 (0.1414)	5.14 · 10 ⁻⁵ (12.33)	0.0000 (2149.21)	x	x		x	x	x	x	x	x	x
Minimum TLC [s]	0.7129 (0.1202)	0.8454 (0.1202)	0.8296 (0.1034)	1.1071 (0.1628)	1.1693 (0.2032)	1.1900 (0.1454)	5.7413e-04 (8.81)	1.1102e-16 (483.14)	x	x					x	x	x	x
<i>Workload:</i>																		
NASA-TLX [%]	40.2083 (14.4447)	27.2569 (12.8877)	32.1875 (13.6816)	29.7222 (14.1478)	23.8194 (14.1889)	23.5764 (11.9643)	8.7791e-04 (8.2335)	8.5967e-05 (22.5996)	x						x			x
SWRR [s ⁻¹]	0.7207 (0.1685)	0.5788 (0.1120)	0.6473 (0.1560)	0.6378 (0.1842)	0.5362 (0.1209)	0.5949 (0.1380)	2.43 · 10 ⁻⁴ (10.02)	1.94 · 10 ⁻⁴ (19.60)	x			x			x			x
Mean abs driver torque [Nm]	1.1806 (0.0856)	1.4779 (0.1016)	1.6038 (0.0935)	1.0859 (0.0788)	1.5326 (0.1807)	1.4271 (0.0769)	2.4425e-14 (84.70)	2.9553e-05 (30.65)	x	x		x	x		x			x
Mean abs feedback torque [Nm]	-	0.5884 (0.1186)	0.5812 (0.1070)	-	0.7218 (0.1916)	0.4540 (0.0956)	9.76 · 10 ⁻⁶ (31.77)	0.8516 (0.0358)	-	-		-	-		x			x
<i>Acceptance:</i>																		
VDL acceptance [-]	-	0.7667 (0.5027)	0.6417 (0.6540)	-	0.6417 (0.4717)	0.6333 (0.5459)	0.6326 (0.2347)	0.3353 (0.9684)	-	-		-	-		-			-
VDL satisfaction [-]	-	0.3958 (0.9750)	0.6250 (0.7590)	-	0.5833 (0.9659)	0.8542 (0.6507)	0.2813 (1.2172)	0.0411 (4.6843)	-	-		-	-		-			-

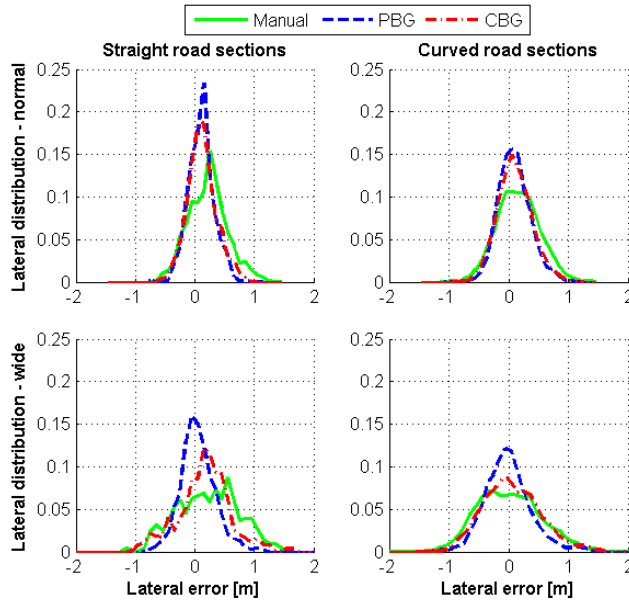


Fig. 5: Distribution of lateral position on the road, averaged over all participants, for road width 3 m (top figures) and road width 5 m (bottom figures), on straight sections (left figures) and curved road sections (right figures). Depicted are manual driving (green, solid), driving with Performance-Based Guidance (blue, dashed), and driving with Criticality-Based Guidance (red, dash-dot). Bin size was 0.1 m.

A. Performance

Figure 5 depicts the mean lateral distributions of all three guidance conditions for the normal road and the wide road. On the normal road, both Performance-based guidance (PBG) and Criticality-based guidance (CBG) improve lane keeping performance compared to manual driving, with reduced variability in lateral position. This effect is visible for both straight and curved road sections. Conversely, on the wide road, PBG continues to offer improvement, but the lateral distribution of CBG more closely matches manual driving. This effect was more pronounced in curved road sections.

From table 1, lane keeping performance in terms of both mean absolute lateral error and peak lateral error was significantly improved over the entire road, for both PBG and CBG on both the normal and wide road, compared to manual driving. No difference between either guidance condition was discovered on the normal road. On the wide road, no difference in peak lateral error was found between both guidance conditions; however, PBG significantly reduced mean absolute lateral error, compared to CBG. All three driving conditions significantly increased both mean absolute lateral error and peak lateral error, as function of road width. No significant interaction effect between guidance condition and lane width was discovered for peak lateral error; all three guidance conditions yielded similar relative changes, from normal to wide road width. On the other hand, mean absolute lateral error

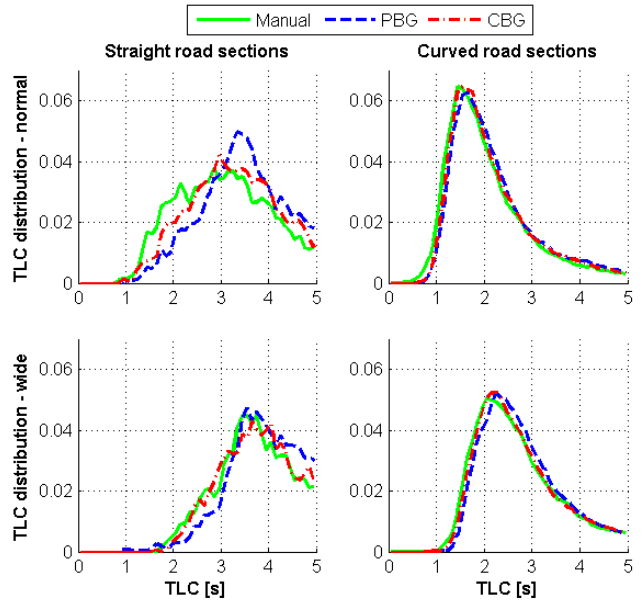


Fig. 6: Distribution of TLC, averaged over all participants, for road width 3 m (top figures) and road width 5 m (bottom figures), on straight sections (left figures) and curved road sections (right figures). Depicted are manual driving (green, solid), driving with Performance-Based Guidance (blue, dashed), and driving with Criticality-Based Guidance (red, dash-dot). Bin size was 0.1 s.

yielded a significant effect of interaction; guidance condition altered performance differently for changing road width.

B. Safety Margins

Figure 6 visualizes the average distribution of TLC (bin size 0.1 s) for all driving conditions. On straight road sections, at normal road width (top left figure), manual driving has the highest distribution at low TLC; on the other hand, PBG has the highest safety margins. This difference is much less pronounced on the wide road (bottom left). For curved road sections, all three driving conditions yield similar distribution profiles, regardless of lane width (top right, bottom right). TLC is strongly influenced by curvature, which explains the relative lack of influence of guidance condition. This is supported by figure 8: variability between subjects is small for curved road sections, compared to straight road sections.

Analysis over the entire normal road profile yielded significantly improved overall safety margins for both guidance conditions, in terms of median TLC, compared to manual driving. No significant difference between the two guidance conditions was discovered. On the wide road, PBG yielded significantly improved overall safety margins, compared to both manual driving and CBG. The most critical driving situation, measured as lowest TLC, was significantly improved by both guidance conditions on the normal road. Comparison of PBG and CBG did not yield significant differences. On

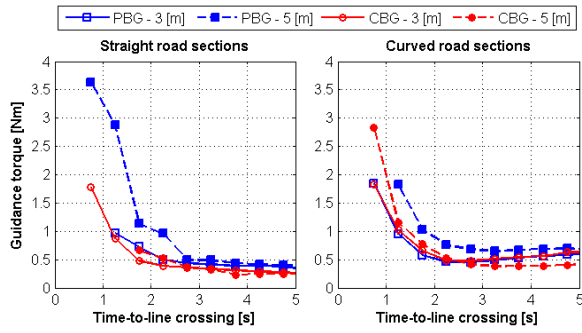


Fig. 7: Guidance torques, as a function of time-to-line crossing, for performance-based guidance (PBG, blue) and criticality-based guidance (CBG, red) on both normal road width (3 m, solid) and wide road width (5 m, dashed). TLC was binned in sections of 0.5 s and plotted against corresponding average guidance torque. The left figure visualizes response on straight road sections, the right figure depicts response in curved road sections. Not all participants recorded equally low TLC values; data points can be the average of less than 24 participants. If no values were recorded for a bin, it was left empty.

the wide road, no difference between any of the three driving conditions was discovered. As expected, both TLC metrics significantly increased as function of road width. However, no significant interaction effect was discovered; TLC margins changed equally for all three driving conditions, as function of road width.

C. Workload

Self reported workload, in terms of NASA-TLX %, was reduced significantly by PBG, compared to manual driving, on the normal road. Comparison with CBG, as well as all comparisons within the wide road, did not yield significant differences. However, both manual driving and CBG did yield a significant reduction in workload, when comparing the normal road condition to the wide road; this was captured in the significant interaction effect. Evaluation of steering wheel reversal rate (SWRR) yielded similar results as the analysis of NASA-TLX: a significant reduction was reported for PBG compared to manual driving, for both road widths. Moreover, SWRR was significantly reduced for manual driving on the wide road, compared to the normal road. Analysis did not yield a significant interaction effect.

Visualized in figure 7 are mean feedback torques at corresponding safety levels, in terms of time-to-line crossing. TLC was divided into bins of 0.5 s; if no TLC values were recorded for a bin by any participant, it was left empty. Driving with road width 3 m yielded similar guidance torques as function of TLC, for both PBG and CBG. On the wide road, PBG yielded higher torques than CBG; this effect was consistent for both straight and curved road sections.

Over the entire road, mean absolute driver torque yielded significant differences for all pairwise comparisons, except for the comparison between PBG and CBG on the wide road, and

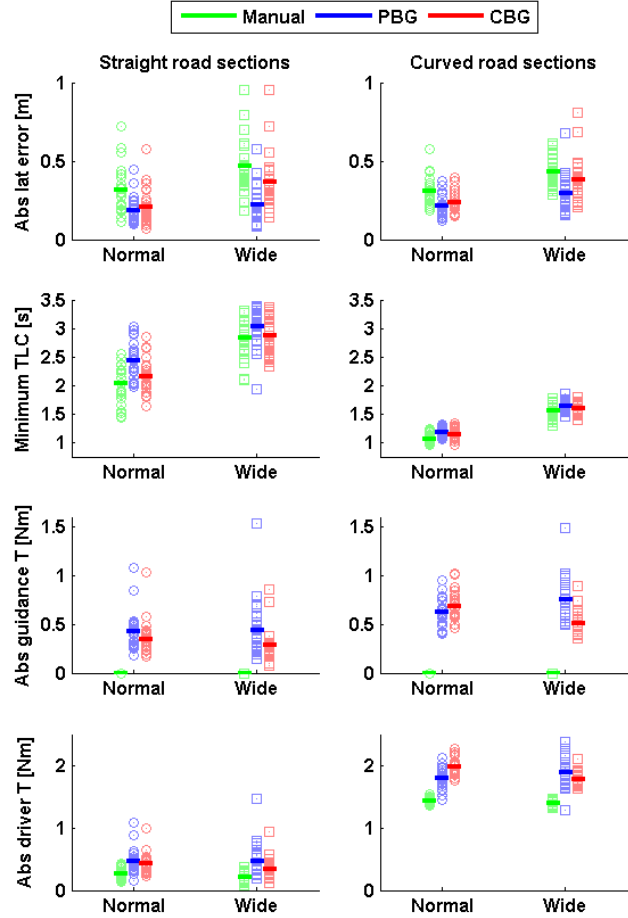


Fig. 8: Individual result and average result for all participants for mean absolute lateral error, minimum TLC, mean absolute feedback torque and mean absolute driver torque. Left column corresponds to metric on straight road sections; right column corresponds to curved road sections. Circles and squares denote individual response on normal road width (3 m) and wide road width (5 m), respectively; single values were collected by averaging response for a single condition (6 and 12 repetitions for straight and curved road sections, respectively). Horizontal bars correspond to the average over all participants, for manual driving (green), PBG (blue) and CBG (red).

comparison between the different road widths for PBG. On the both road widths, drivers had to exert higher torques with both PBG and CBG, compared to manual driving. Moreover, the use of CBG resulted in significant higher driver torques on the normal road, compared to PBG. Both manual driving and CBG significantly lowered the driver torques in a comparison between the normal and wide road, which was captured by the significant interaction effect of the 2-way ANOVA.

Comparing PBG and CBG over the entire road, no significant difference was discovered for guidance torques on

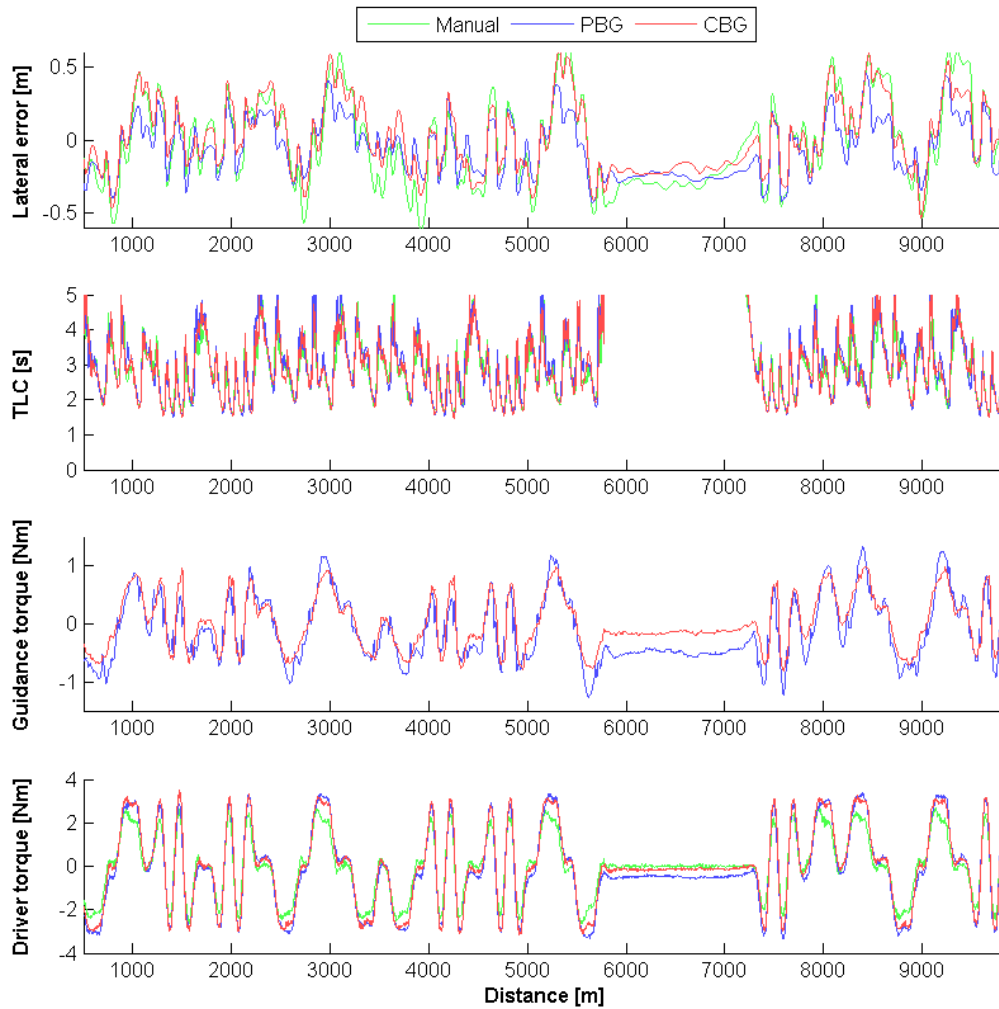


Fig. 9: Average response over 24 participants for lateral error, TLC, guidance torque and driver torque, as function of distance (road width = 5 m).

the normal road width. However, CBG offered significantly less guidance torques on the wide road, compared to PBG. Moreover, PBG significantly increased feedback torques from the normal road to the wide road; conversely, CBG yielded a significant reduction in feedback torques. On straight road sections, guidance torques were lower for CBG, compared to PBG (figure 8). On curved road sections, PBG yielded lower guidance torques on the normal road width than CBG, but higher torques on the wide road width. The same trend is visible for driver torques.

The ratio between increase in driver torque, compared to manual driving, and corresponding guidance torque was investigated to quantify conflict levels (Saleh et al., 2013). On average, PBG resulted in an additional 0.5053 and 0.6189 Nm of driver torque, for every Nm of guidance torque provided

(normal and wide road, respectively). Analysis of CBG returned a ratio of 0.7281 and 0.7515.

D. System Acceptance

No significant effect of guidance type was discovered for either self-reported acceptance or satisfaction. Lane width did not influence acceptance, although guidance was considered more satisfying on the wide road by participants.

V. DISCUSSION

A. Benefits of haptic steering guidance

The aim of this research was to investigate the benefits and limitations of the CBG, compared to both manual driving and current haptic guidance systems, as task difficulty changes. On

the normal road, a clear benefit in performance was achieved with both guidance conditions, compared to manual driving; participants were able to follow the center of the road more accurately, and the largest excursion was reduced. Moreover, safety margins were significantly improved with both guidance conditions; for average driving (calculated as median TLC) and the most critical situation (minimum TLC), time margins were improved. Besides improvements in performance and safety margins for both guidance systems, performance-based guidance also achieved a reduction in workload; both subjective (NASA-TLX) and objective (SWRR) measures indicated reduced workload. These benefits for performance-based guidance are in line with results of previous studies (referred to therein as continuous guidance; Mulder et al., 2012; Melman et al., 2017). However, both PBG and CBG yielded a significant increase in driver torques, thereby potentially mitigating some of the objective workload benefits. Interestingly, no improvements in workload were reported for criticality-based guidance. Although it provides continuous guidance torques, a large portion of these torques are presented at highly critical situations; as such, participants were supported with low levels of guidance torques through the majority of the task. In Petermeijer et al. (2014), drivers were supported only after surpassing a lateral error threshold. A similar lack of workload benefits was reported, compared to manual driving; this was due to participants mostly driving manually throughout the task, by staying within the bandwidth. Although both guidance systems increase guidance torque non-linearly as the vehicle deviates from the centerline, the increase in driver torques reported by Petermeijer et al. (2014) was relatively small compared to torques exerted during manual driving; on the other hand, CBG yielded a large increase in driver torques. This did not reflect in driver acceptance of the guidance system: no difference between PBG and CBG was reported for usefulness or satisfaction.

B. Conflict

The reduction in guidance torques for CBG on the wide road, compared to the normal road width, corresponded with a significant reduction in driver torques. However, despite the significantly lower feedback torques on the wide road, compared to PBG, driver torques were not significantly lowered. The ratio between additional driver torques and feedback torques illustrates a mismatch between driver trajectory and corresponding guidance system trajectory; participants were more likely to be in disagreement with CBG, compared to PBG. A possible explanation of this artifact is the reduced reliance of the driver on the guidance system; PBG offers support regardless of road width, instigating driver reliance on the system and a corresponding increase in driver compliance. On the other hand, CBG offers relatively more freedom; possibly, drivers are more likely to ignore low guidance torques, only giving way to high guidance torques. This effect of driver compliance was investigated by Flemisch et al. (2014) and Petermeijer et al. (2014): at higher level of haptic authority, drivers were more reliant on the support system, and less likely to maintain vigilance.

C. Human-like driving

An increase in human-like deviation from the lane centerline, as visualized in figure 5, was achieved for CBG on the wide road, compared to PBG. The importance of identifying and supporting natural human driving, within boundaries of acceptable driving, has been argued by Saleh et al. (2011), Boer (2016) and Kolekar et al. (2016). This presents a trade-off: supporting natural human driving behavior versus improving performance and safety margins. As such, determining the appropriate level of (haptic) authority of support systems has been the topic of ample research (Abbink et al., 2011; Mars et al., 2014; Parasuraman et al., 1999; Flemisch et al., 2014). The use of criticality-based guidance supports drivers in time critical situations, but allows for natural human deviation as task safety improves, such as curve cutting (figures 5 and 9).

D. Guidance as-needed

The benefits of PBG on the wide road, in terms of performance, safety margins and workload, come at the cost of increased guidance torque; this is regardless of safety levels (see figure 7). As task difficulty decreases (due to increasing lane width) PBG offers increased guidance torques. However, literature points towards decreasing guidance in less difficult or less critical tasks, to encourage drivers to maintain cognitive engagement (Brookhuis and de Waard, 1993; De Visser et al., 2008; Sheridan and Parasuraman, 2002). The adverse effects of (unnecessarily) high guidance torques include speeding (Melman et al., 2017), increased vulnerability to automation failure (Flemisch et al., 2014; Petermeijer et al., 2014), and even diminished performance benefits (Mars et al., 2014).

On the other hand, CBG adheres to the principle of guidance as-needed: the adjustment of support to task requirements or measurements (Miller et al., 2005). Guidance as-needed often contains a dead zone, in which no guidance torques are presented (De Winter and Dodou, 2011; Petermeijer et al., 2014). However, this paper has presented an alternative: a continuous, non-linear increase of guidance-torques in increasingly critical situations. This offers the advantage of improved system functionality, as continuous interaction between driver and support system is facilitated (Abbink et al., 2011). Indeed, binary switching control authority was considered 'annoying and difficult to interpret' by participants (Petermeijer et al., 2014).

The lower guidance torques of CBG, compared to PBG, did not result in deteriorated safety margins. Neither the largest excursion (peak lateral error) nor the most time critical situation (minimum TLC) was improved. CBG thus achieved similar improvements in safety, whilst reducing the aforementioned limitations of haptic steering guidance systems.

E. Limitations and future work

This study was conducted on a fixed based driving simulator. However, curve cutting behavior serves to limit lateral acceleration (Boer, 2016); as such, larger excursions are expected in motion based simulators or in real world driving. The inclusion of traffic will increase task complexity and improve

generalizability; it also allows for the inclusion of time-to-collision, developing a more complete support system (Mulder et al., 2011).

Parameter identification can be revisited, in order to reduce conflict torques by more closely matching human control action. The parameter structure also allows for individualization; the adaptation of control parameters to a single driver, to yield improved cooperation in terms of steering wheel angles (Boink et al., 2014).

Recent research (Melman et al., 2017) shows that haptic steering guidance can result in speeding, mitigating safety benefits of the support system. The designed CBG controller increases guidance torques at increased velocity, due to the reduced time margins. Future research should investigate criticality-based guidance in a longitudinal driving simulation study to quantify these effects.

VI. CONCLUSION

Criticality-based steering guidance is a viable alternative to conventional, performance-based guidance. Benefits in terms of performance and safety margins have been discovered in a critical driving task. Moreover, guidance decreases when risks of driving are diminished, thereby presenting guidance as-needed; this is achieved without compromising the improvement in safety margins. These advantages are at the cost of increased driver torques: the authors encourage future research into individualization of parameters or other techniques to reduce conflict torques.

ACKNOWLEDGMENT

The authors would like to thank Timo Melman for his contributions. David Abbink and Sarvesh Kolekar are supported by the Netherlands Organization for Scientific Research (NWO), VIDI project 14127.

REFERENCES

- Abbink, D. A. and Mulder, M. (2009). Exploring the Dimensions of Haptic Feedback Support in Manual Control. *Journal of Computing and Information Science in Engineering*, 9(1):1–9.
- Abbink, D. A., Mulder, M., and Boer, E. R. (2011). Haptic shared control: smoothly shifting control authority? *Cognition, Technology & Work*, 14(1):19–28.
- Boer, E. R. (2016). Satisficing Curve Negotiation: Explaining Drivers' Situated Lateral Position Variability. *IFAC-PapersOnLine*, 49(19):183–188.
- Boink, R., van Paassen, M. M., Mulder, M., and Abbink, D. A. (2014). Understanding and reducing conflicts between driver and haptic shared control. *2014 IEEE International Conference on Systems, Man, and Cybernetics*, pages 1510–1515.
- Brookhuis, K. A. and de Waard, D. (1993). The use of psychophysiology to assess driver status. *Ergonomics*, 36(9):1099–1110.
- Byrne, E. A. and Parasuraman, R. (1996). Psychophysiology and adaptive automation. *Biological Psychology*, 42:249–268.
- De Groot, S., De Winter, J. C. F., López-García, J. M., Mulder, M., and Wieringa, P. A. (2011). The Effect of Concurrent Bandwidth Feedback on Learning the Lane-Keeping Task in a Driving Simulator. *Human Factors*, 53(1):50–62.
- De Nijs, S. (2011). The power of haptic guidance. *Master's thesis, TU Delft, Delft University of Technology*, pages 1–12.
- De Visser, E., LeGoullon, M., Freedy, A., Freedy, E., Weltman, G., and Parasuraman, R. (2008). Designing an adaptive automation system for human supervision of unmanned vehicles: A bridge from theory to practice. *Proceedings of the Human Factors and Ergonomics Society 52nd Annual Meeting*, pages 221–225.
- De Winter, J. C. F. and Dodou, D. (2011). Preparing drivers for dangerous situations: A critical reflection on continuous shared control. *Conference Proceedings - IEEE International Conference on Systems, Man and Cybernetics*, pages 1050–1056.
- Della Penna, M., Van Paassen, M. M., Abbink, D. A., Mulder, M., and Mulder, M. (2010). Reducing steering wheel stiffness is beneficial in supporting evasive maneuvers. *Conference Proceedings - IEEE International Conference on Systems, Man and Cybernetics*, pages 1628–1635.
- Flemisch, F. O., Bengler, K., Bubb, H., Winner, H., and Bruder, R. (2014). Towards cooperative guidance and control of highly automated vehicles: H-Mode and Conduct-by-Wire. *Ergonomics*, 57(3):343–60.
- Forsyth, B. A. C. and MacLean, K. E. (2006). Predictive haptic guidance: intelligent user assistance for the control of dynamic tasks. *IEEE transactions on visualization and computer graphics*, 12(1):103–13.
- Goodrich, M. A., Stirling, W. C., and Boer, E. R. (2000). Satisficing revisited. *Minds and Machines*, 10(1):79–110.
- Griffiths, P. and Gillespie, R. (2004). Shared control between human and machine: haptic display of automation during manual control of vehicle heading. *Proceedings of the 12th International Symposium on Haptic Interfaces for Virtual Environment and Teleoperator Systems*, pages 358–366.
- Hart, S. G. and Staveland, L. E. (1988). Development of NASA-TLX (Task Load Index): Results of Empirical and Theoretical Research. *Advances in Psychology*, 52(C):139–183.
- Kolekar, S. B., Mugge, W., and Abbink, D. A. (2016). A Human-like steering model based on sensorimotor control theories. *Master's thesis, TU Delft, Delft University of Technology*, pages 1–12.
- Mars, F., Deroo, M., and Hoc, J. M. (2014). Analysis of human-machine cooperation when driving with different degrees of haptic shared control. *IEEE transactions on haptics*, 7(3):324–33.
- Melman, T., de Winter, J. C. F., and Abbink, D. A. (2017). Does haptic steering guidance instigate speeding? A driving simulator study into causes and remedies. *Accident Analysis and Prevention*, 98:372–387.
- Miller, C. A., Funk, H. B., Goldman, R. P., Meisner, J., and Wu, P. (2005). Implications of Adaptive vs. Adaptable UIs on Decision Making: Why 'Automated Adaptiveness' Is Not Always the Right Answer. *Proceedings of the 1st International Conference on Augmented Cognition*, pages

- 1180–1189.
- Mohellebi, H., Kheddar, A., and Espié, S. (2009). Adaptive Haptic Feedback Steering Wheel for Driving Simulators. *IEEE Transactions on Vehicular Technology*, 58(4):1654–1666.
- Mulder, M., Abbink, D. A., and Boer, E. R. (2008). The effect of haptic guidance on curve negotiation behavior of young, experienced drivers. *2008 IEEE International Conference on Systems, Man and Cybernetics*, pages 804–809.
- Mulder, M., Abbink, D. A., and Boer, E. R. (2012). Sharing Control With Haptics: Seamless Driver Support From Manual to Automatic Control. *Human Factors: The Journal of the Human Factors and Ergonomics Society*, 54(5):786–798.
- Mulder, M., Abbink, D. A., Van Paassen, M. M., and Mulder, M. (2011). Design of a Haptic Gas Pedal for Active Car-Following Support. *IEEE Transactions on Intelligent Transportation Systems*, 12(1):268–279.
- Nudehi, S., Mukherjee, R., and Ghodoussi, M. (2005). A shared-control approach to haptic interface design for minimally invasive telesurgical training. *IEEE Transactions on Control Systems Technology*, 13(4):588–592.
- Okamura, A. and Li, M. (2003). Recognition of operator motions for real-time assistance using virtual fixtures. *Proceedings of the 11th Symposium on Haptic Interfaces for Virtual Environment and Teleoperator Systems*, pages 125–131.
- Parasuraman, R., Mouloua, M., and Hilburn, B. (1999). Adaptive aiding and adaptive task allocation enhance human-machine interaction. In *Automation technology and human performance: Current research and trends*, pages 119–123.
- Petermeijer, S. M., Abbink, D. A., and de Winter, J. C. F. (2014). Should Drivers Be Operating Within an Automation-Free Bandwidth? Evaluating Haptic Steering Support Systems With Different Levels of Authority. *Human Factors: The Journal of the Human Factors and Ergonomics Society*, 57(1):5–20.
- Rajamani, R. (2006). Vehicle Dynamics and Control. In *Mechanical engineering series*, pages 257–285. Springer.
- Saleh, L., Chevrel, P., Claveau, F., Lafay, J. F., and Mars, F. (2013). Shared steering control between a driver and an automation: Stability in the presence of driver behavior uncertainty. *IEEE Transactions on Intelligent Transportation Systems*, 14(2):974–983.
- Saleh, L., Chevrel, P., Mars, F., Lafay, J. F., and Claveau, F. (2011). Human-like cybernetic driver model for lane keeping. *IFAC Proceedings Volumes*, 18(1):4368–4373.
- Sheik-Nainar, M. A., Kaber, D. B., and Chow, M. Y. (2005). Control Gain Adaptation in Virtual Reality Mediated Human–Telerobot Interaction. *Human Factors and Ergonomics in Manufacturing*, 15(3):259–274.
- Sheridan, T. B. and Parasuraman, R. (2002). Human-Automation Interaction. pages 89–129.
- Tsoi, K. K., Mulder, M., and Abbink, D. A. (2010). Balancing safety and support: Changing lanes with a haptic lane-keeping support system. *Conference Proceedings - IEEE International Conference on Systems, Man and Cybernetics*, pages 1236–1243.
- Van Der Horst, R. (2004). Occlusion as a measure for visual workload: An overview of TNO occlusion research in car driving. *Applied Ergonomics*, 35:189–196.
- Van Der Laan, J., Heino, A., and De Waard, D. (1997). A simple procedure for the assessment of acceptance of advanced transport telematics. *Transportation Research Part C: Emerging Technologies*, 5(1):1–10.
- Van Winsum, W., Brookhuis, K. A., and De Waard, D. (2000). A comparison of different ways to approximate time-to-line crossing (TLC) during car driving. *Accident Analysis and Prevention*, 32(1):47–56.
- Van Winsum, W. and Godthelp, H. (1996). Speed choice and steering behavior in curve driving. *Human factors*, 38(3):434–441.
- Wilson, G. F., Russell, C. A., and Davis, I. (2006). The Importance of Determining Individual Operator Capabilities When Applying Adaptive Aiding. *Proceedings of the Human Factors and Ergonomics Society 50th Annual Meeting*, (1):141–145.
- Zhai, S., Accot, J., and Woltjer, R. (2004). Human Action Laws in Electronic Virtual Worlds: An Empirical Study of Path Steering Performance in VR. *Presence: Teleoperators and Virtual Environments*, 13(2):113–127.